Journal of Southeast University (English Edition) Vol. 30, No. 3, pp. 348 - 352 Sept. 2014 ISSN 1003—7985

Influence of different curing regimes on the microstructure and macro performance of UHPFRCC

Saly Fathy Sun Wei

(School of Materials Science and Engineering, Southeast University, Nanjing 211189, China)

Abstract: This study investigates the influence of different curing regimes on the microstructure and macro properties of ultra-high performance fiber reinforced cementitious composite (UHPFRCC), and aims to discover whether it is possible to produce qualified UHPFRCC using different curing regimes. A control mix of UHPFRCC is prepared. The mechanical performance and the short-term durability of the UHPFRCC matrix under three curing regimes are studied. In addition, the microstructures of the UHPFRCC matrix with different curing conditions are analyzed by combining scanning electron microscopy (SEM) and mercury intrusion porosimetry (MIP). The results explore how different UHPFRCC curing regimes affect its microstructure and how the microstructure affects its macro behavior. Heat and steam curing for 3 d is succeeded to produce the UHPFRCC with nearly the same mechanical properties and durability as those of the 90 d standard curing. However, the heat cured UHPFRCC does not show great resistance to chloride-ion penetration.

Key words: ultra-high performance fiber reinforced cementitious composite (UHPFRCC); curing regimes; durability; microstructure

doi: 10.3969/j.issn.1003 - 7985.2014.03.017

The development of material properties is the basis for the design and construction of structures made from cement-based materials [1]. Applying appropriate curing methods is essential for any concrete to gain properties, particularly for UHPFRCC. Like all other concretes, UHPFRCCs require water to hydrate, but compared to other concretes, UHPFRCCs have been engineered to require very little water. The reduced water content in the UHPFRCC mix necessitates careful attention to curing practices so as not to allow the included water to escape prior to hydration [2]. In practical engineering applications, the cases of the in-situ concrete applications and the pre-cast elements are both required. This explains the importance of studying the availability of the production of UHPFRC using both different curing regimes (rapid and standard curing). Refs. [3 - 4] showed the effect of curing conditions on the mechanical properties of UHPFRCC. This study presents the influence of different curing regimes not only on the macro performance but also on the micro structure of UHPFRCC produced with different curing conditions, using scanning electron microscopy (SEM) and mercury intrusion porosimetry (MIP).

1 Experimental

1.1 Materials

The early strength Portland cement (PC) used in the experiments is produced by Jiangnan Cement Co., Ltd., Nanjing and it is classified as P. II 52.5R according to the Chinese standards. The physical and mechanical properties of the materials are shown in Tab. 1. Grade Ⅰ fly ash (FA), similar to Class F fly ash according to ASTM, is supplied by the Zhenjiang Power Plant with a specific surface area of 454 m^2/kg. The silica fume (SF) used in the experiments is produced by the Ai Ken Company with a specific surface area of 22 000 m^2/kg. The oxide compositions of the FA and SF analyzed with the X-ray fluorescence spectroscopy are listed in Tab. 2.

Ordinary river sand with a maximum diameter of 2.36 mm, a fineness modules of 2.44, and a packing and apparent density of 1.4 and 2.4 g/cm^3, respectively, is used as fine aggregates. A visconcrete 3301 superplasticizer (SP) supplied by the Switzerland Sika (China) Building Materials Co., Ltd. with a water reducing ratio of more than 30% and a solid content of 28% is used. Dramix, a superfine steel fiber covered by a copper, is incorporated. The fibers (VF) are 13 mm long and have a circular cross-section with a diameter of 0.2 mm.

1.2 Mix proportion

The mix design of UHPFRC differs significantly from that of normal and high-strength concretes [5]. UHPFRCC mix compositions are characterized by: 1) The enhancement of homogeneity by elimination of coarse aggregates; 2) The enhancement of compacted density by optimization of the granular mixture, i.e. silica fume improves the compacted density of the mix, thereby reducing voids

Received 2013-12-12.

Biographies: Saly Fathy (1985—), female, graduate; Sun Wei (corresponding author), female, professor, academician of China Engineering Academy, sunwei@seu.edu.cn.

Foundation items: The Scholarship Supported by the China Scholarship Council, the Technical Research Program from NV Bekaert SA of Belgium, the National Natural Science Foundation of China (No. 50908047).

Citation: Saly Fathy, Sun Wei. Influence of different curing regimes on the microstructure and macro performance of UHPFRCC[J]. Journal of Southeast University (English Edition), 2014, 30(3): 348 - 352. [doi: 10.3969/j.issn.1003 - 7985.2014.03.017]

Tab. 1 Physical and mechanical properties of cement

Standard consistency/%	Initial setting time/min	Final setting time/min	Flexural strength/MPa		Compressive strength/MPa		Specific surface area/($m^2 \cdot kg^{-1}$)
			3 d	28 d	3 d	28 d	
26.3	140	245	7.2	10.6	34.7	62.8	362

Tab. 2 Oxide compositions of FA and SF %

Mineral admixture	$w(SiO_2)$	$w(Al_2O_3)$	$w(Fe_2O_3)$	$w(CaO)$	$w(MgO)$	$w(SO_3)$	$w(K_2O)$	$w(Na_2O)$	Loss
FA	54.88	26.86	6.49	4.77	1.31	1.16	1.05	0.88	2.5
SF	94.48	0.27	0.83	0.54	0.97	0.8			2.13

and defects; 3) The reduction of the water/cement ratio and inclusion of a superplasticizer which ensures a workable mix; 4) The enhancement of ductility by incorporating small-sized steel fibers. The composition of the prepared UHPFRCC matrix is shown in Tab. 3.

Tab. 3 Mixing proportion of UHPFRCC kg/m^3

Cement	Fly ash	Silica fume	River sand	Superplasticizer	Water	Steel fiber
540	432	108	1296	37.8	172.8	160

1.3 Specimen preparation

The main step in specimen preparation is to produce a uniform distribution of UHPFRCC components including binder materials and steel fibers. Therefore, according to the mixture proportions in Tab. 3, fresh concrete mixtures are cast into steel molds to produce samples with a dimension of 40 mm × 40 mm × 160 mm, and then placed on a shaking table in order to achieve good compaction. After the samples are kept for 24 h at room temperature, the prism specimens are demoulded and cured with different curing regimes. For standard curing, the temperature is at (20 ± 2) ℃, and has a relative humidity RH greater than 95%. For steam curing specimens, the specimens are put into a steam box of 85 ℃ for 3 d, and as to the heat curing specimens, they are put into an oven at 105 ℃ for 3 d.

1.4 Test method

1.4.1 Mechanical properties test method

According to the Chinese standard GB/T 17671—1999, the bending specimen is a prism (40 mm × 40 mm × 160 mm) when applying a three-point bending test. The span is 100 mm, and the loading rate is 1 mm/min. The compressive strength specimen is a 40 mm × 40 mm × 40 mm cube.

1.4.2 Durability test method

In this study, the chloride analysis is undertaken according to the Chinese standard JTJ 270—1998 and the NT Build 443—94 [6]. After taking the specimens from the curing rooms, each specimen is coated with gas-tight epoxy resin. One surface of each specimen is left uncoated for the purpose of exposing this surface to a NaCl solution[7]. The UHPFRCC specimens are placed with a 10% NaCl solution for 2, 3, 4 months, respectively. Immediately after the specified immersion period, the specimens are taken out and dried for 2 d at (60 ± 30)°C. Powder samples are collected from depths of 0 to 5 mm, 5 to 10 mm, 10 to 15mm and 15 to 20 mm. Using a drill, at least 5 g of fine powder are extracted from each depth. Subsequently, the chloride content, as a percentage of Cl^- by the mass of concrete, is determined by titration.

The freeze-thaw test is conducted according to GB/T 50082—2009. The test data are collected once after every 25 freeze-thaw cycles to determine the weight-loss rate and the relative dynamic elastic modules of the specimens.

2 Results and Discussion

2.1 Mechanical properties

2.1.1 Effect of curing regimes on mechanical properties of UHPFRCC

The data in Fig. 1 represent the flexural and compressive strength of the cured UHPFRCC under the three curing regimes (standard curing, heat curing and steam curing). From this data it can be concluded that fast heat curing for 3 d can make UHPFRCC exhibit close mechanical properties to those of 90 d standard curing.

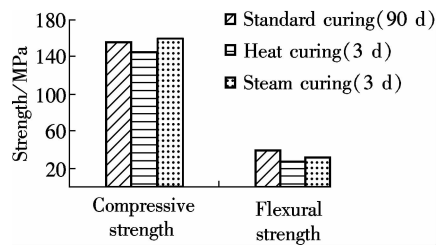

Fig. 1 Mechanical properties of UHPFRCC subjected to different curing regimes

Steam curing at 85 ℃ and heat curing at 100 ℃ for 3 d are used to enhance UHPFRCC properties by accelerating the hydration reaction of cement particles and the Pozzolanic reaction of the mineral admixtures including silica fume and fly ash, and then to achieve high early strength it can be used for precast elements. However, UHPFRCC cured in standard conditions ((20 ± 2) ℃, RH > 95%) without heat treatment successfully gains sufficient strength, to be able to be used in situ applications for rehabilitation and strengthening of structures[8].

When comparing the strength results of 3 d heat and steam curing, it is found that at the same age, the

strength of steam cured specimens is greater than that of heat cured specimens. This is because in dry hot conditions, water evaporates easily, which leads to the formation of a small number of large pores and results in a slight increase in materials porosity and, thus, strength slightly decreases.

2.1.2 Effect of curing regimes on the toughness of UHPFRCC

Load-deflection curves of the three systems of 90 d standard curing, 3 d heat curing and 3 d steam curing are shown in Fig. 2.

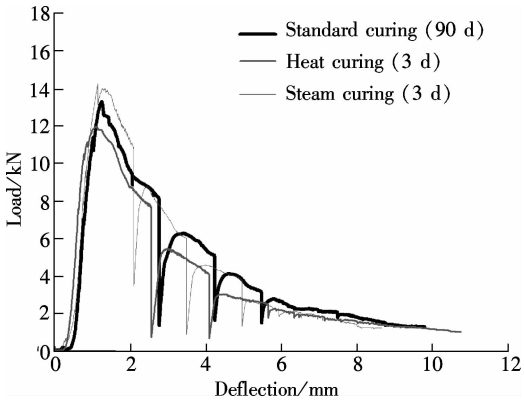

Fig. 2 Load-deflection curves of UHPFRCC under different curing conditions

The damage produced by the expansion caused by the hot and the humid conditions of dry hot and steam curing, respectively, was decreased due to the addition of steel fibers. The incorporation of steel fibers in UHPFRCC matrix increases the resistance to hot and humid expansion stress.

Fig. 2 shows that the steam curing for UHPFRCC after 3 d has the greatest toughness among the three curing regimes. That is because the Pozzolanic materials become more reactive under high temperature conditions, which makes the strength of the UHPFRCC increase quickly. On the other hand, the slurry water evaporates due to the high temperature conditions, resulting in the formation of a small number of large pores which can slightly reduces the strength. However, in the steam curing, the steam compensates for the humidity loss.

2.2 Results for the durability tests

2.2.1 Chloride resistance of UHPFRCC with different curing regimes

Fig. 3 shows the Cl^- concentration distribution at different depths in UHPFRCC150 with different curing conditions after 90 d immersion. It can be concluded that the Cl^- diffusion concentration value for the heat cured UHPFRCC specimens at the 5 to 10 mm depth is five times more than that for the steamed and standard cured UHPFRCC at the same depth. When using heat curing, the water evaporates from the matrix, leaving some connected internal pores and leading to the easy and quick penetration of the chloride ions into UHPFRCC. Most of chloride concentrations of the standard curing with steam curing matrices concentrate only at the 0 to 5 mm depth. Compared to the standard curing, steam curing matrices have better resistance to chloride ion penetration. This means that steam curing can speed up the hydration process of UHPFRCC and lead to a dense microstructure in a shorter time which is even more efficient than the 90 d standard curing.

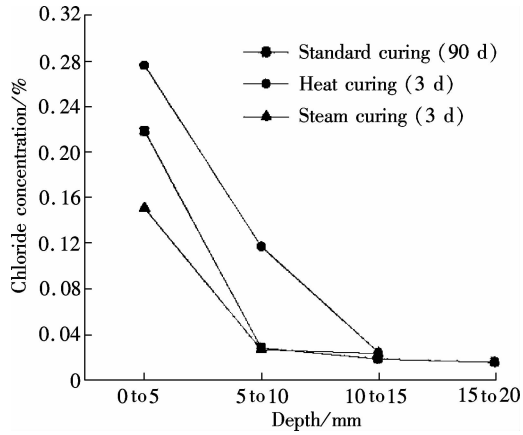

Fig. 3 Chloride concentrations at different depths of UHPFRCC with different curing conditions after 90 d immersion

2.2.2 Effects of curing condition on the freeze-thaw performance of UHPFRCC

Figs. 4 and 5, respectively, show the effects of curing regimes on the mass loss and the relative dynamic modulus of elasticity of UHPFRCC with the increase of freeze-thaw cycles. For the three different curing regimes and after 800 cycles of freezing and thawing, the mass loss and the relative dynamic elastic modules are about 1.0% and 95%, respectively. The results of the heat and steam curing do not differ much from the standard curing results. This means that the rapid curing has no significant influence on the UHPFRCC frost resistance.

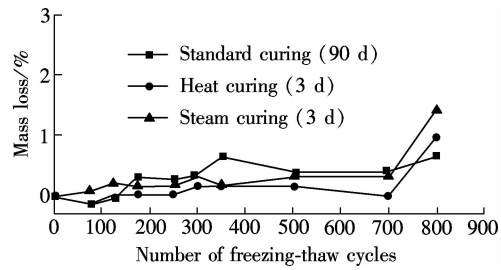

Fig. 4 Effects of curing condition on the mass loss of UHPFRCC

2.3 Results of microstructure tests

As MIP provides information about the connectivity of the pores and microscopy reveals information about pore geometry, researchers have been interested in combining the techniques for a more complete picture of pore systems[9].

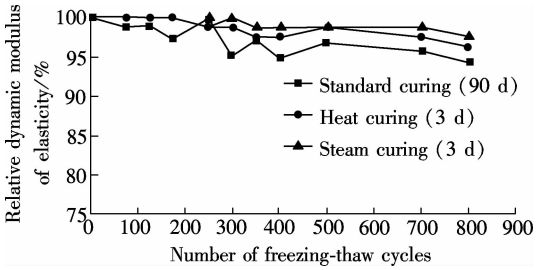

Fig. 5 Effect of curing conditions on relative dynamic modulus of elasticity of UHPFRCC

2.3.1 Morphology of UHPFRCC after different curing regimes

Figs. 6 and 7 shows the morphology of UHPFRCC after 3 d heat curing and steam curing, respectively. No obvious Ca $(OH)_2$ exists in UHPFRCC, which indicates that the hydration process in UHPFRCC has been almost completed after a short time of the heat or steam curing. For heat curing regimes, because of the high temperature, water evaporates from the specimens and leaves small connected pores as can be seen in the figures. The chlorides can penetrate into UHPFRCC very fast through the connected pores. This is the reason why heat cured UHPFRCC has relatively lower mechanical properties and chloride resistance than the other two curing regimes. On the contrary, for steam curing, steam compensates for the loss of water from the UHPFRCC matrix's surface, which leads to a more smooth and dense microstructure. In addition, standard cured UHPFRCC has a similar morphology to steam cured UHPFRCC.

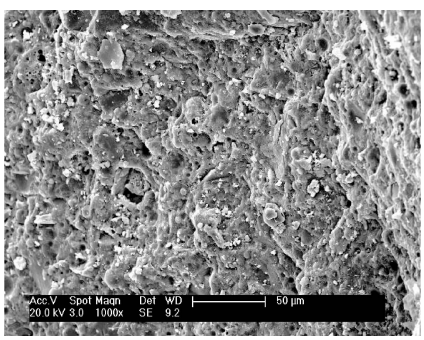

Fig. 6 The SEM image of UHPFRCC after heat curing

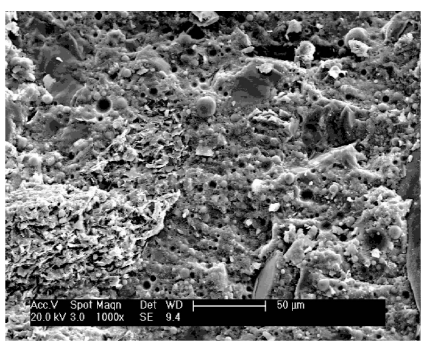

Fig. 7 The SEM image of UHPFRCC after steam curing

2.3.2 Effects of curing condition on the pore size distribution of UHPFRCC

Fig. 8 is the pore size distribution of UHPFRCC with the three different curing regimes. The figure shows that the most probable pore size in the three groups of specimens is about 4 to 5 nm, indicating that the pores in the UHPFRCC matrix are mainly small size gel pores, which are harmless for the mechanical performance and durability of UHPFRCC. It is also obvious that the heat cured UHPFRCC has higher porosity. For heat curing, there are many pores with sizes between 10 and 100 nm in UHPFRCC. This also indicates that the water evaporates out of specimens during the curing, and leaves connected pores in UHPFRCC as seen in the SEM image. These pores reduce the chloride resistance of heat cured UHPFRCC.

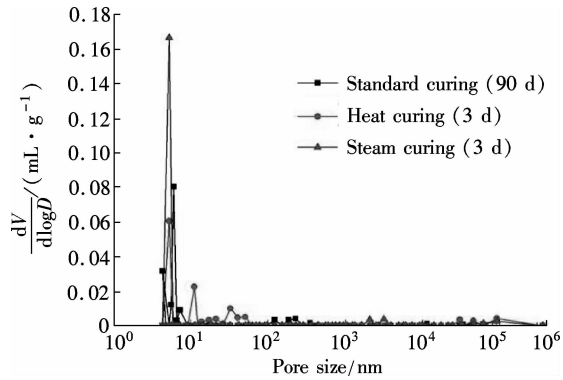

Fig. 8 Effects of curing condition on the pore size distribution of UHPFRCC

3 Conclusion

The research shows that UHPFRCC can be produced successfully with three different regimes. The rapid curing condition can serve the case of pre-cast elements, and the results indicate the possibility of producing UHPFRCC using standard curing to be able to be used in situ applications for rehabilitation and strengthening of structures. The results show the effects of the different curing regimes not only on the macro behavior of UHPFRCC but also on its micro structure. Combining the advanced methods of testing the microstructure of the UHPFRCC matrix including SEM and MIP can produce a more complete understanding of the reasons for the excellent performance of UHPFRCC.

References

[1] Hong K N, Kang S T, Kim S W, et al. Material properties of air-cured ultra-high-performance steel-fiber-reinforced concrete at early ages[J]. *International Journal of the Physical Sciences*, 2010, **5**(17): 2622 - 2634.

[2] Graybeal B. Ultra-high performance concrete, FHWA-HRT-11-038 [R]. Mclean, VA, USA: Federal Highway Administration, 2011.

[3] Yang S, Millard S, Soutsos M, et al. Influence of aggre-

gate and curing regime on the mechanical properties of ultra-high performance fibre reinforced concrete (UHPFRC) [J]. *Construction and Building Materials*, 2009, **23**(6): 2291 - 2298.
[4] Yazici H. The effect of curing conditions on compressive strength of ultra high strength concrete with high volume mineral admixtures [J]. *Building and Environment*, 2007, **42**(5): 2083 - 2089.
[5] Habel K, Viviani M, Denarié E, et al. Development of the mechanical properties of an ultra-high performance fiber reinforced concrete (UHPFRC) [J]. *Cement and Concrete Research*, 2006, **36**(7): 1362 - 1370.
[6] Nordtest. Concrete hardened: accelerated chloride penetration, NT Build 443 [R]. Espoo, Finland: Nordtest, 1995.
[7] Zhang Y S, Sun W, Chen S D, et al. One and two dimensional chloride ion diffusion of fly ash concrete under flexural stress [J]. *Journal of Zhejiang University: SCIENCE A*, 2011, **12**(9): 692 - 701.
[8] Habel K, Charron J P, Braike S, et al. Ultra-high performance fibre reinforced concrete mix design in central Canada [J]. *Canadian Journal of Civil Engineering*, 2008, **35**(2): 217 - 224.
[9] Abell A B, Willis K L, Lange D A. Mercury intrusion porosimetry and image analysis of cement-based materials [J]. *Journal of Colloid and Interface Science*, 1999, **211**(1): 39 - 44.

养护制度对超高性能纤维增强水泥基复合材料微观结构及宏观性能的影响

Saly Fathy　孙　伟

(东南大学材料科学与工程学院, 南京 211189)

摘要: 研究了不同养护制度对超高性能纤维增强水泥基复合材料(UHPFRCC)微观结构和宏观性能的影响,并揭示了用不同的养护制度制备性能符合要求的超高性能纤维增强水泥基复合材料的可能性. 制备了一种基准的 UHPFRCC,研究了 3 种养护制度下 UHPFRCC 的力学性能及短期耐久性能. 此外,通过结合运用电子扫描电镜(SEM)和压汞法(MIP),测试了 3 种养护制度下 UHPFRCC 的微观结果. 研究结果揭示了不同的养护制度对 UHPFRCC 微观结构的影响以及微观结构对材料宏观性能的影响机制. 热养护和蒸汽养护 3 d 与标准养护 90 d 的 UHPFRCC 具有相近的力学性能和耐久性. 但是,热养护的 UHPFRCC 具有相对较差的抗氯离子渗透性能.

关键词: 超高性能纤维增强水泥基复合材料;养护制度;耐久性;微观结构
中图分类号: TU528